



2013-12-01

FGF4 Induced Wnt5a Gradient in the Limb Bud Mediates Mesenchymal Cell Directed Migration and Division

John C. Allen

Brigham Young University - Provo

Follow this and additional works at: <https://scholarsarchive.byu.edu/etd>

 Part of the [Cell and Developmental Biology Commons](#), and the [Physiology Commons](#)

BYU ScholarsArchive Citation

Allen, John C., "FGF4 Induced Wnt5a Gradient in the Limb Bud Mediates Mesenchymal Cell Directed Migration and Division" (2013). *All Theses and Dissertations*. 4309.

<https://scholarsarchive.byu.edu/etd/4309>

This Thesis is brought to you for free and open access by BYU ScholarsArchive. It has been accepted for inclusion in All Theses and Dissertations by an authorized administrator of BYU ScholarsArchive. For more information, please contact scholarsarchive@byu.edu, ellen_amatangelo@byu.edu.

FGF4 Induced Wnt5a Gradient in the Limb Bud
Mediates Mesenchymal Cell Directed
Migration and Division

John C. Allen

A thesis submitted to the faculty of
Brigham Young University
in partial fulfillment of the requirements for the degree of
Master of Science

Jeffery R. Barrow, Chair
Michael R. Stark
Laura C. Bridgewater

Department of Physiology and Developmental Biology
Brigham Young University
December 2013

Copyright © 2013 John C. Allen
All Rights Reserved

ABSTRACT

FGF4 Induced Wnt5a Gradient in the Limb Bud

Mediates Mesenchymal Cell Directed

Migration and Division

John C. Allen

Department of Physiology and Developmental Biology, BYU

Master of Science

The AER has a vital role in directing embryonic limb development. Several models have been developed that attempt to explain how the AER directs limb development, but none of them are fully supported by existing data. I provide evidence that FGFs secreted from the AER induce a gradient of Wnt5a. I also demonstrate that limb mesenchyme grows toward increasing concentrations of Wnt5a. We hypothesize that the changing shape of the AER is critical for patterning the limb along the proximal to distal axis. To better understand the pathway through which Wnt5a elicits its effects, we have performed various genetic studies. We demonstrate that Wnt5a does not signal via the Wnt/ β -catenin pathway. However, we show that Wnt5a mutants share many common defects with Vangl2 mutants suggesting that Wnt5a signals through the Wnt/planar cell polarity (PCP) pathway.

Keywords: FGF4, AER, apical ectodermal ridge, Wnt5a, Wnt5b, Wnt3a, limb, Ror2, Ror1, Ryk, PCP, planar cell polarity, neural tube, vangl2, looptail

ACKNOWLEDGEMENTS

I would like to thank Dr. Jeffery Barrow for being my mentor, for providing guidance in the lab, but also for spiritual guidance and for his kind words during hard times. I'd like to thank my committee for their direction. Most of all, I want to recognize my family: my mother, who wanted me to earn my master's degree more than I did so she wouldn't be the only one with graduate degrees; my dad, who wanted me to be successful even if he didn't see the benefit of graduate school; my brothers, who kept me motivated in a way that only brothers can: by making fun of me and punching me and even sometimes giving me words of encouragement. Last of all, I am especially grateful for my friend Benjamin the dog who reminded me to take the occasional walk to sniff the grass and scratch his head and who may have furtively accompanied me to the lab in the middle of the night.

TABLE OF CONTENTS

TITLE PAGE	i
ABSTRACT	ii
ACKNOWLEDGEMENTS	iii
TABLE OF CONTENTS.....	iv
LIST OF FIGURES	vi
LIST OF TABLES	vii
INTRODUCTION.....	1
Apical Ectodermal Ridge.....	1
Figure 1: The apical ectodermal ridge (AER)	1
Figure 2: AER removal at later stages results in more distal truncations	1
Figure 3: Mesenchyme recombination experiments.....	2
Models for Limb Development	3
Figure 4: The Progress Zone Model and the Early Specification Model.....	3
The Limb Mesenchyme Recruitment Model	5
Figure 5: Changes in AER shape during development.....	5
Figure 6: Labeled mouse limb cells exhibiting outgrowth.....	6
Figure 7: Labeled cells directly proximal to regions of removed AER.....	7
Figure 8: Chick limb development after removal of the AER	8
FGFs.....	9
Wnt5a.....	10
Figure 9: Progressive Wnt5a expression in the limb	10
Figure 10: Wnt5a expression in Wnt3; Msx2-Cre mice	10
Figure 11: Wnt5a expression in wildtype and mutant mice.....	11
Planar Cell Polarity.....	11
Figure 12: PCP pathway signaling components.....	13
Figure 13: Neural tube defects exhibited in PCP mutants	14
Figure 14: Convergent extension in wild type and PCP mutants.....	14
Figure 15: Wnt5a/5b mutant defects.....	15
PROPOSAL	16
Hypothesis.....	16
Objectives and Overview	16
Specific aim #1	16
FGF4 induction of Wnt5a	16
Wnt5a induction of directed cell migration:	17
Specific Aim #2	17
Wnt5a signaling through β -catenin pathway:.....	17
Convergent extension defects of midline cells in Wnt5a/Wnt5b mutants:.....	18
Length-to-width ratios of Wnt5a/Wnt5b mutants:	18
Neural tube cell polarity defects:.....	19
RESULTS	20
FGF4 induction of Wnt5a expression.....	20
Figure 16: Wnt5a induction in response to varying concentrations of FGF4	20
Figure 17: Directed mesenchymal cell migration in response to Wnt5a.....	21

Wnt5a signaling through the PCP pathway	21
Figure 18: Wnt5a/Wnt5b mutants maintain β -catenin signaling	22
Figure 19: Wnt5a/Wnt5b and Vangl2 mutants have similar CE defects	23
Figure 20: Length to width ratios	24
Table 1: Neural tube defects in Wnt5a/Wnt5b and looptail mutants.....	25
DISCUSSION	26
METHODS	31
Windowing eggs	31
Wnt5a Bead Implants.....	31
FGF Bead Implants.....	31
Mouse Strains and Genotyping	32
<i>in situ</i> Hybridization	32
X-gal Staining.....	33
Length-to-Width Ratio (LWR) Measurement in Neurulating Embryos.....	33
Embryo Collection, Embedding, and Sectioning	34
Immunohistochemistry	34
WORKS CITED.....	36
CURRICULUM VITAE.....	41

LIST OF FIGURES

Figure 1: The apical ectodermal ridge (AER)	1
Figure 2: AER removal at later stages results in more distal truncations	1
Figure 3: Mesenchyme recombination experiments	2
Figure 4: The Progress Zone Model and the Early Specification Model.....	3
Figure 5: Changes in AER shape during development	5
Figure 6: Labeled cells directly proximal to regions of removed AER.....	7
Figure 7: Labeled mouse limb cells exhibiting outgrowth along the proximodistal axis	6
Figure 8: Chick limb development after removal of the AER and FGF4 bead placement	8
Figure 9: Progressive Wnt5a expression in the limb	10
Figure 10: Wnt5a expression in Wnt3; Msx2-Cre mice which exhibit variable AER loss.....	10
Figure 11: Wnt5a expression in wildtype and mutant mice	11
Figure 12: PCP pathway signaling components	13
Figure 13: Neural tube defects exhibited in PCP mutants.....	14
Figure 14: Convergent extension in wild type and PCP mutants	14
Figure 15: Wnt5a/5b mutant defects.....	15
Figure 16: Wnt5a induction in response to varying concentrations of FGF4	20
Figure 17: Directed mesenchymal cell migration in response to Wnt5a	21
Figure 18: Wnt5a/Wnt5b mutants maintain β -catenin	22
Figure 19: Wnt5a/Wnt5b and Vangl2 (looptail) mutants have similar CE defects	23
Figure 20: Length to width ratios of various Wnt5a/Wnt5b and looptail genotypes.....	24

LIST OF TABLES

Table 1: Neural tube defects in Wnt5a/Wnt5b and looptail mutants.....	25
---	----

INTRODUCTION

Apical Ectodermal Ridge

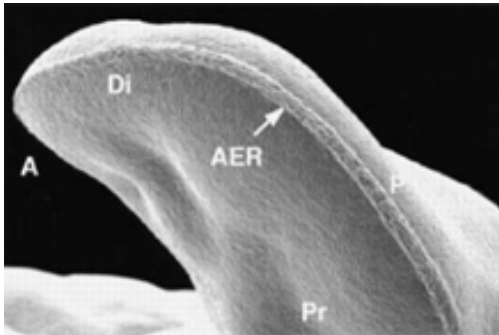


Figure 1: The apical ectodermal ridge (AER)

The embryonic limb consists of an ectodermal jacket surrounding loosely-packed mesoderm. The ectoderm develops into epidermis and epidermal appendages while the underlying limb mesoderm develops into the limb skeleton, and tendons. At the distal margin of the vertebrate embryonic limb there is a ridge of tissues that is called the apical ectodermal ridge (AER, figure 1). In a landmark experiment, John Saunders removed the AER of embryonic chick limbs to determine its function. He found that AER removal at early embryonic stages results in severe distal truncations of the embryonic limb, and that removing the AER at progressively later stages results in increasing restoration of distal structures (figure 2). These results demonstrate that the AER is crucial regulating distal outgrowth of the limb mesenchyme and patterning it distally as a function of time (Saunders 1948).

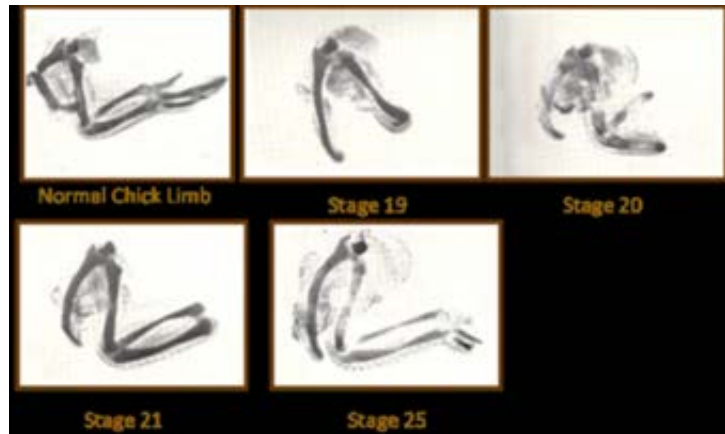


Figure 2: AER removal at later stages results in more distal truncations (Saunders 1948)

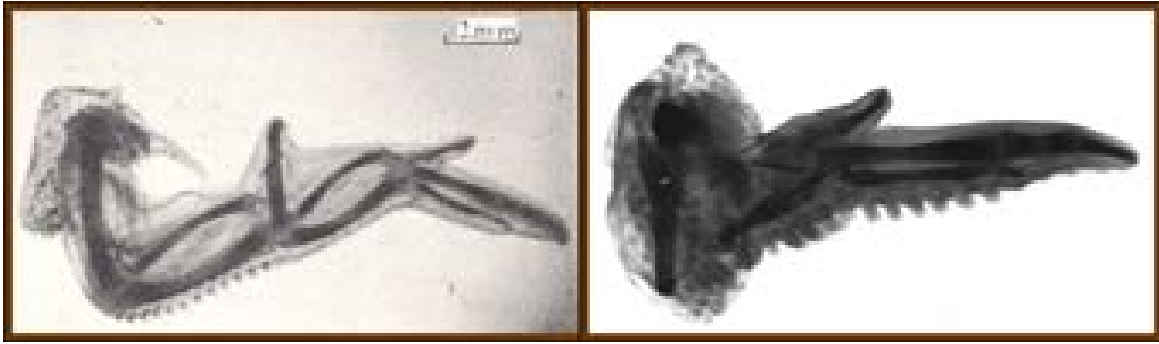


Figure 3: Mesenchyme recombination experiments. (Left) Earlier AER and distal mesenchyme on a later limb bud. (Right) Later AER and distal mesenchyme on an earlier limb bud (Summerbell and Lewis 1975)

Saunders first proposed that the mechanism whereby the AER patterns the limb distally over time was due to changes in instructive signals secreted from the AER as time progressed. To test this hypothesis, Saunders grafted the AER of young limb buds onto the distal mesenchyme of older limb buds, and the AER of old limb buds onto the mesenchyme of young limb buds (Rubin and Saunders 1972)(figure 3). He found that the age of the AER did not affect limb pattern. Saunders therefore determined that the AER sends a permissive signal that is critical for limb outgrowth but is not instructive for the development of structures along the proximal to distal axis.

Later researchers theorized that the underlying mesenchyme possesses the proximal to distal pattern information. To test this hypothesis, Summerbell et al., transplanted the AER and the underlying distal mesenchyme from old limb buds to young limb buds, and vice versa. They found that when distal mesenchyme from earlier-stage embryos was transplanted to later-stage embryos, that the earlier structures were replicated. When later-stage distal mesenchyme and AER was transplanted to earlier stage limb buds, distal structures formed without proximal structures (Summerbell, Lewis and Wolpert 1973)(figure 3). From these results Summerbell and colleagues proposed that all cells that are within signaling range of the AER constitute the “progress zone”. Later experiments demonstrated that FGF4 is the permissive signal that is

secreted from the AER (Niswander et al. 1993). Using beads that were soaked in FGF4, proper proximal to distal limb bud patterning was restored when the AER was removed (Niswander et al. 1993).

Models for Limb Development

Researchers conducting the AER and distal mesenchyme transplant experiments theorized that limb patterning information was found in the mesenchyme (Summerbell and Lewis 1975, Summerbell et al. 1973). Their findings provided the basis for the Progress Zone Model of limb development which proposes that the fate of cells along the proximodistal axis is specified by the length of time that the cells spend in the progress zone (i.e., the mesenchymal cells within signaling range (i.e., 200 μm) of the AER (figure 4A). The putative signal received by these cells from the AER allows them to continue proliferating and remain undifferentiated. As these cells proliferate, some are pushed out of the progress zone and differentiate. Cells that are pushed out early take on a proximal fate, while cells that remain in the progress zone longer will take on a more distal fate. This model proposes the cells in the progress zone have an internal timer that determines the identity of mesenchymal cells based on how long they remain

in the progress zone. The AER allows this timer to continue operating. When the cells fall out of the progress zone, the timer stops, and the cell's fate is set. In Saender's AER transplant experiments, young AER grafted to old limbs and old

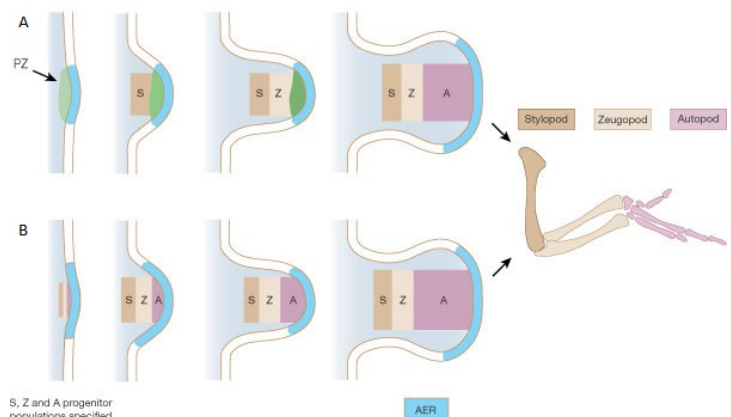


Figure 4: The Progress Zone Model (A) and the Early Specification Model (B) (Mariani and Martin 2003)

AER grafted to young limbs developed normal limb patterns. Both young and old AER are sending the same permissive signal to the mesenchyme.

The progress zone model remained the only viable model to describe how the AER patterns the limb proximodistally for many years. In 2003, a second model was put forth that could better account for some novel data that refuted the PZ model (Moon and Capecchi 2000, Lewandoski, Sun and Martin 2000). The Early or Pre-Specification Model proposes that there are 3 pre-specified regions in the early limb bud that give rise to the stylopod, which corresponds with the humerus, the zeugopod - radius and ulna, and the autopod, - hand or foot (figure 4B). Cells take on a stylopod, zeugopod, or autopod fate early in development (Dudley, Ros and Tabin 2002), and not as the cells fall out of the progress zone. The AER sends a signal to the limb bud that activates outgrowth and proximodistal expansion as development progresses. When the AER is removed, all cells within 200 μm of the AER undergo apoptosis. The stage of development when the AER is removed determines which of the pre-specified zones are still within 200 μm of the AER and will therefore not develop. Another finding that supports this model is that when cells at different distances from the AER are labeled early in limb development, these cells are restricted to a single segment of the limb.

Neither of these models can fully explain all of the experimental data for limb development. There is also no molecular evidence that supports these models (Tabin and Wolpert 2007). Another model is needed to fully explain vertebrate limb development and patterning.

The Limb Mesenchyme Recruitment Model

Previous data collected in our lab suggests a different model for AER-mediated outgrowth and patterning of the limb mesenchyme along the proximodistal axis. We propose that FGFs from the AER induce expression of a Wnt5a gradient in the adjacent limb mesenchyme. This Wnt5a gradient provides a directional cue to mesenchymal cells through a pathway involving the Wnt5a receptor (Ror2)(Yoda, Oishi and Minami 2003). These cells are recruited to growth towards the AER via directed migration or oriented cell divisions.

If the AER recruits mesenchyme in its direction then its dimensions will be important to shape mesenchymal cells that are recruited toward it. We have observed that shape of the AER changes over time in a way that mirrors the shape of the limb skeleton. For example, shortly after its induction the AER is circular (figure 5A, 5B). A circular AER would be predicted to recruit a cylindrical mass of mesenchyme that would condense to form the stylopod. Over time the AER elongates along the anteroposterior (AP) and thins along the dorsoventral (DV) axis, (figure 5C, 5D) (Barrow et al. 2003, Litingtung et al. 2002, Barrow Unpublished) which would be predicted to recruit a thin paddle-shaped mass of mesenchyme prefiguring the shape of the autopod. Consistent with this model are data from various mutants that exhibit defects in the shape of the AER. For example, the conditional Wnt3a knockout mouse $Wnt3^{n/c}; RARCre$ exhibits a reduced AER along the anterior-posterior axis (Barrow et al. 2003). These mice exhibit severe oligodactyly. In

contrast, *Gli3* mutants which possess an AER that much longer than in controls exhibit

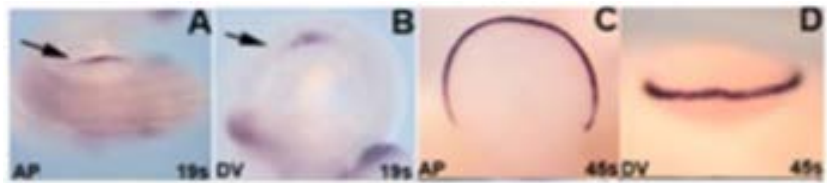


Figure 5: Changes in AER shape during development (Barrow Unpublished)

an extra wide limb bud and polydactyly (Litingtung et al. 2002).

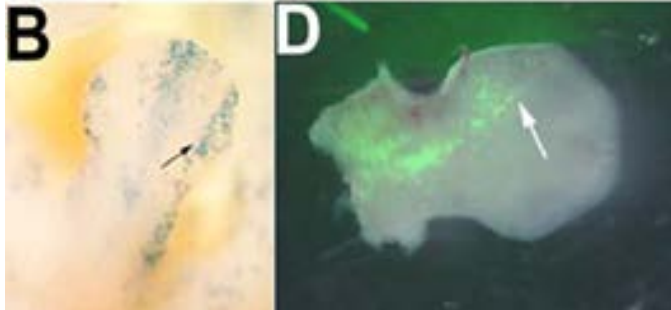


Figure 6: Labeled mouse limb cells exhibiting outgrowth along the proximodistal axis (Sowby and Barrow Unpublished)

Research done in the Barrow lab supports the Limb Mesenchyme Recruitment model. Labeled cells were found to grow directionally toward the AER, instead of forming a circular clone, evidence of directional growth (Sowby

and Barrow Unpublished, Mao et al. 2005). Cell labeling studies done in chick limbs confirm this data. In these studies, labeled clones elongate towards the AER, indicating that directed outgrowth is occurring (figure 6) (Dudley et al. 2002, Li and Muneoka 1999, Vargesson et al. 1997).

Removal of portions of the AER disrupts outgrowth of adjacent mesenchyme (figure 7). Cells adjacent to the regions with removed AER either redirect their growth toward remaining AER or form a radial clone if they are too far away from any AER (Kendall et al. Unpublished). Slight indentations in the limb mesenchyme that enlarge over time are observed near removed AER regions. Explanations for these findings from other models of limb development include decreases in cellular proliferation or increases in apoptosis (Dudley et al. 2002). According to the Limb Mesenchyme Recruitment model, cells are not being recruited towards areas of removed AER; they are growing toward adjacent remaining AER.

Previous experiments done in the Barrow lab involving loss of AER have also revealed a loss of Wnt5a signaling (Barrow et al. 2003). Wnt5a has a demonstrated role in directed migration and cell growth (He et al. 2008, Yamaguchi et al. 1999a, Wyngaarden et al. 2010, Gros et al. 2010) and is expressed as a gradient in the distal tip of the mesenchyme (Barrow et al. 2003).

Transplanted Wnt5a-soaked beads have

demonstrated an ability to redirect growth of mesenchymal limb cells (Wyngaarden et al. 2010, Gros et al. 2010).

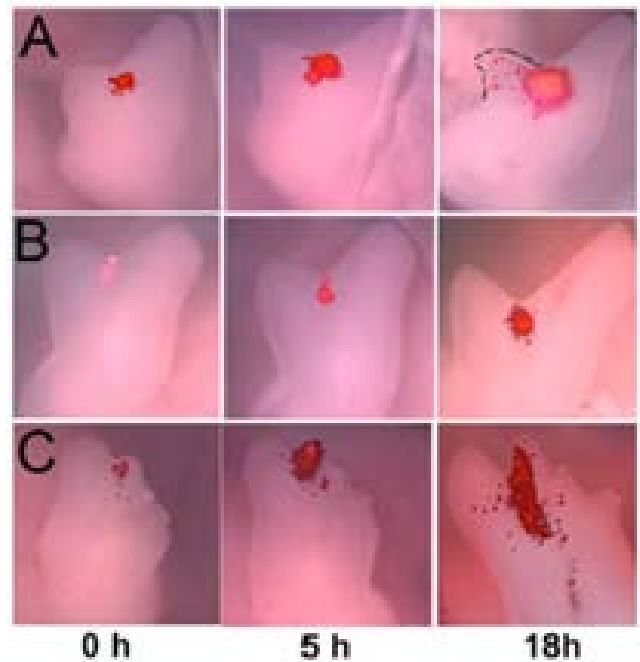


Figure 7: Labeled cells directly proximal to regions of removed AER (Kendall et al. Unpublished)

Supporting the Limb Mesenchyme Recruitment Model is the demonstrated ability of the changing shape of the AER to change the morphology of the limb from the proximal to the distal end. To do this, the AER expresses Fgf4, which in turn induces the expression of a Wnt5a gradient. This Wnt5a gradient establishes a proximodistal cell orientation and mediates the directed growth of limb mesenchymal cells toward the AER, which is necessary for development of the vertebrate limb. (Barrow et al. 2010, Wyngaarden et al. 2010, Gros et al. 2010).

However, some experimental data indicates that additional signaling is present in the distal limb bud. Using Fgf4 beads to replace the AER (Niswander et al. 1993) (figure 8), researchers found that either one or two beads placed on the posterior side of the developing limb bud were able to stimulate limb growth. Patterning, however, was disturbed. The round beads, shaped similarly to the very early AER, directed stylopod growth fairly normally. Since these

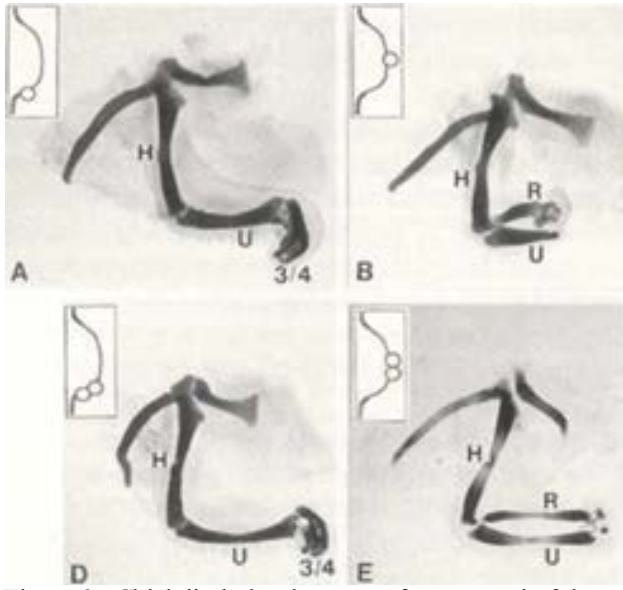


Figure 8: Chick limb development after removal of the AER and placement of an Fgf4 bead (Niswander et al. 1993)

beads cannot change shape over time as the AER does, therefore the spherical bead induces a stylopod-shaped zeugopod. This finding is consistent with the hypothesis that the shape of the AER will dictate the shape of the mesenchyme and therefore the skeletal element that forms.

This model predicts that in the autopod, a single, thickened digit would develop.

However, digits did develop, but they

developed in a circular cluster and all exhibited a posterior character (digit 3 or 4, figure 8D).

The cylindrically arranged digits correspond with the round shape of the Fgf4 bead as predicted by the Limb Mesenchyme Recruitment Model. The development of separated digit elements instead of one thick digit does not, however, indicate that some distal signal is present that is separate from the AER. This signal imparts a polarizing message to the cells of the distal limb mesenchyme, enabling digits to develop that are different from anterior to posterior.

When beads were placed on the apical ectoderm, development of the limb stopped at certain points. One bead produced a relatively normal humerus, but outgrowth of the limb stopped in the middle of the zeugopod, producing only half of the radius and ulna. Placing two beads on the apical ectoderm produced a normal radius and ulna, but development halted before the autopod developed. Since development in limbs with posterior beads did not halt, this indicates that some the signal is produced by the posterior mesenchyme that allows digit development in the autopod.

FGFs

Much work has been done to determine what secreted factors are responsible for the limb outgrowth and patterning activity of the AER. Several FGFs are expressed by the AER (Crossley and Martin 1995, Niswander and Martin 1992). To determine whether these FGFs could replace the limb outgrowth and patterning activity of the AER, the AER was removed and replaced with FGF2 and FGF4 soaked beads. The beads were able to rescue proximal to distal limb pattern, although there are defects in the shapes of bones along the anteroposterior (AP) and dorsoventral (DV) axes (Cohn et al. 1995, Fallon et al. 1994, Niswander et al. 1993).

FGF8 also has a role in limb outgrowth (Crossley and Martin 1995). Limb-specific knockouts of FGF4 and FGF8 in mice demonstrate loss of limb development due to failure of mesenchymal cells to survive (Boulet et al. 2004, Sun, Mariani and Martin 2002). Limb-specific knockouts of FGF8 lack a humerus/femur, but not distal skeletal elements (Moon and Capecchi 2000, Lewandoski et al. 2000). Other experiments show that the limb-specific *Msx2-Cre*; FGF4; FGF8 mutant forelimbs lack anterior components such as the radius and anterior autopod, while hind limbs fail to develop entirely (Sun et al. 2002). Because Cre is expressed earlier in the hindlimb than in the forelimb, expression of FGF4 and FGF8 is knocked out earlier, which causes the hindlimb failure to develop which the only distal forelimb components fail to develop. Limb-specific FGF4/FGF8 mutants do not exhibit cell death in the distal limb bud, only proximally at later stages far from the AER where FGFs are secreted (Sun et al. 2002).

Additionally, FGFs act as a chemoattractant, inducing mesenchymal cells to grow towards the AER. Mesenchymal cells are induced to divide and migrate towards an FGF4-soaked bead that was implanted in the limb (Saxton et al. 2000, Li and Muneoka 1999, Niswander et al. 1993). FGF4 has no influence on cell orientation, directed mitosis, or directed

movement, however, it does increase the velocity of random cell movements on cells that are closer to the FGF4 source (Gros et al. 2010). As mesenchymal cells move up the FGF4 gradient, they move faster, creating an overall net movement toward the source of FGF4.

Wnt5a

Wnt5a is a secreted protein that is expressed in gradient fashion at the distal end of the growing limb bud, suggesting that its

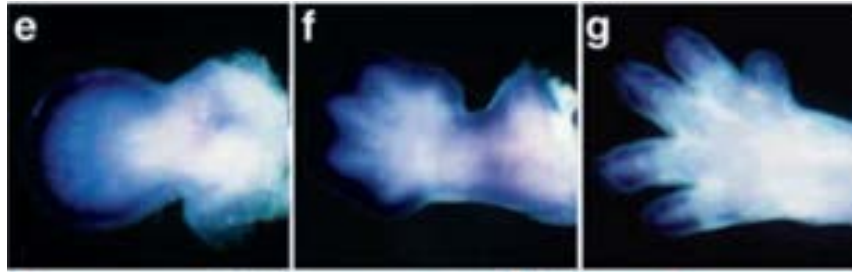


Figure 9: Progressive Wnt5a expression in the limb (Yamaguchi et al. 1999a)

expression may depend on the AER (figure 9) (Yamaguchi et al. 1999a). Indeed, in mutants lacking the AER, there is a concomitant loss of Wnt5a expression (Barrow et al. 2003, Kawakami et al. 1999). The *Wnt3n/c; Msx2-Cre* mouse mutant exhibits a variable loss of the AER (figure 10). Wnt5a expression in mutants appears to be present near regions of residual AER, but not where AER is lost (figure 10) (Barrow et al., 2003). Additional studies that we have done support the hypothesis that Fgf protein may also be sufficient to induce Wnt5a

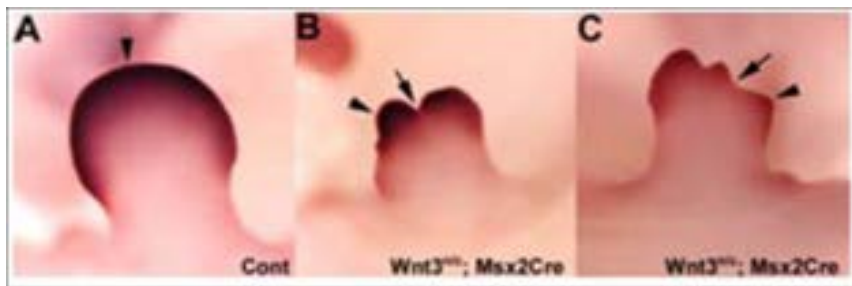


Figure 10: Wnt5a expression in *Wnt3; Msx2-Cre* mice which exhibit variable AER loss. Arrowheads denote AER and arrows denote regions where no AER is present (Barrow Unpublished)

expression in the limb and lateral plate mesoderm. I am rigorously testing this hypothesis presently (see below).

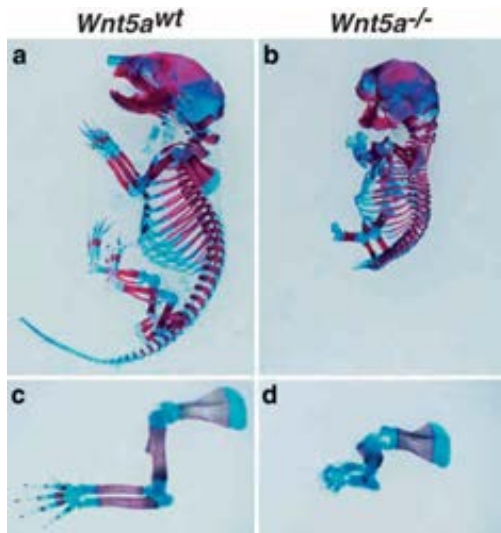


Figure 11: Wnt5a expression in wildtype and mutant mice (Yamaguchi et al. 1999a)

Wnt5a is first expressed in the mouse limb at the 20-22 somite stage (Yamaguchi et al. 1999a) and in the chick at Hamburger-Hamilton stage 14, which corresponds with the initiation of limb bud development (Kawakami et al. 1999, Hamburger and Hamilton 1992). Other structures that exhibit outgrowth, such as the caudal end of the embryo and the face also form a Wnt5a gradient that is concentrated in the direction of outgrowth (figure 11)

(Yamaguchi et al. 1999a). Despite the shortened limbs, face and body axis, Wnt5a still exhibit relatively normal pattern demonstrating in each of these regions (figure 11). Skeletal elements of the limb are progressively truncated proximally to distally and the distal elements do not develop, indicating that mesenchymal cells do not extend along the proximodistal axis (Yamaguchi et al. 1999a). Reduced expression of Wnt5a in fish fin buds was shown to reduce cell migration (Sakaguchi et al. 2006). Other genes involved in limb outgrowth and patterning are still functional, demonstrating a possible loss of the ability of mesenchyme cells to respond to signals from the AER in Wnt5a mutants (Qian et al. 2007, Yamaguchi et al. 1999a). Additionally, retroviral misexpression of Wnt5a in the zeugopod of developing embryos results in shortened long bones, indicating some role in pattern formation (Kawakami et al. 1999).

Planar Cell Polarity

Wnt5a has been shown to play a role in polarizing cell growth and the resulting directed cell movement and oriented cell growth (Heisenberg et al. 2000, Kilian et al. 2003, Qian et al.

2007, Rauch et al. 1997, Westfall et al. 2003, Gong, Mo and Fraser 2004, Barrow 2006, Gros et al. 2010, Wyngaarden et al. 2010). A Wnt5a gradient has been shown to induce a reorganization of the actin cytoskeleton *in vitro* (Witze et al. 2008). Cells of the limb bud are shown to be polarized with the axis of outgrowth, with mitoses and movement oriented distally in a very efficient manner (Gros et al. 2010). However, in Wnt5a mutant limb buds, they demonstrate that distal movement slows down and becomes much less efficient. Cell divisions lose their directionality and cells become more rounded and lose their asymmetry. To show that Wnt5a is acting through the Wnt/polar cell planarity (PCP) pathway, which is responsible for orienting cell divisions and movement in one direction, they treated cultured chick embryos with a PCP pathway inhibitor. These cells behave in a similar manner as the Wnt5a mutant cells, supporting the hypothesis that Wnt5a signals through the PCP pathway to direct limb bud outgrowth (Gros et al. 2010). In a similar study, cells of the lateral plate mesoderm (LPM) at the level of the forelimb are observed to be oriented parallel to the anterior-posterior axis, while limb bud cells are oriented orthogonal to the AP axis and parallel to the proximodistal axis of outgrowth (Wyngaarden et al. 2010). Wnt5a mutant cells of the LPM lose their polarity and oriented mitoses. Cells of the limb bud maintain their directed movements, but at a greatly reduced velocity. Wnt5a mutant mice have a truncated body axis and open neural tube, a similar phenotype to zebrafish that lack components of the PCP pathway (Qian et al. 2007, Yamaguchi et al. 1999a). Wnt5a mutants still develop a normal AER and recognizable proximodistal pattern, suggesting that additional pathways regulate distally oriented growth in vertebrates. Indeed, FGF signaling has been shown to be sufficient to promote directed growth of the limb mesenchyme (Gros et al. 2010).

In the presence of a polarizing signal, such as Wnt5a, core PCP proteins localize to opposite sides of the cell. Dishevelled (Dvl) moves to one side of the cell (Wang et al. 2005, Wang et al. 2006), and Van Gogh-like 2 (Vangl2)

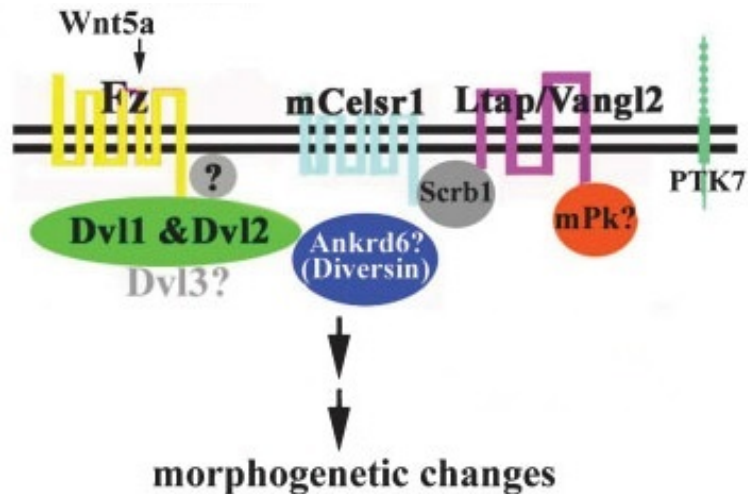


Figure 12: PCP pathway signaling components (Jones and Chen 2007)

moves to the other side (Montcouquiol et al. 2006b). Vangl1, a paralog of Vangl2, may also act as a core PCP protein (Antic et al. 2010, Kibar et al. 2007). Several other proteins are involved in PCP signaling (figure 12).

Several Wnt5a receptors for the PCP pathway have been identified. Wnt5a signals through Ror2, a member of the receptor tyrosine kinase family (Yoda et al. 2003). When bound to Wnt5a, Ror2 forms a ternary complex with Vangl2, which recruits CKI δ and phosphorylates Vangl2, and induces polarized growth via the PCP pathway in the direction of the Wnt5a gradient (Gao et al. 2011). Vangl2 has many serines and threonines which are phosphorylated via Wnt5a signaling. Depending on the concentration of Wnt5a, more of these are phosphorylated. It is possible that the extent of Vangl2 phosphorylation is a way of polarizing cells (Gao et al. 2011). Ryk and Ror1, other members of the receptor tyrosine kinase family may also act as receptors for Wnt5a in PCP signaling (Macheda et al. 2012, Andre et al. 2012, Katoh 2005).

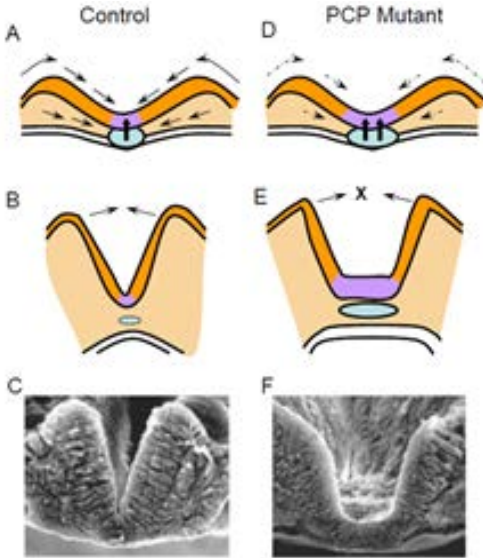


Figure 13: Neural tube defects exhibited in PCP mutants. Neural tube defects are a result of a lack of convergence (D). The notochord (light blue) is broader (D,E) resulting in a broader signal to induce a wide medial hinge point (purple) that exhibits a wide floor plate (E,F), displaying the characteristic U-shape rather than the V-shape found in wild type embryos (E8.5)

There is evidence that the Wnt5a/PCP pathway is also responsible for convergent extension in vertebrates (Montcouquiol, Crenshaw and Kelley 2006a, Wallingford and Harland 2002), a process of mesodermal cells and prechordal plate cells converging medially toward the axial midline, intercalating, and extending the embryonic axis (figure 13) (Copp, Greene and Murdoch 2003, Montcouquiol et al. 2006a, Qian et al. 2007, Ueno and Greene 2003, Wang et al. 2006, Ybot-Gonzalez et al. 2007). This process requires cells to orient in the same direction perhaps similar to how cells must

orient towards the AER for proper limb outgrowth. Neural tube closure is regulated by components of the PCP pathway and is linked to convergent extension of prechordal plate cells (Copp et al. 2003, Doudney and Stanier 2005, Montcouquiol et al. 2006a, Qian et al. 2007, Ueno and Greene 2003, Wang et al. 2006, Ybot-Gonzalez et al. 2007, Wallingford 2006).

Neural tube closure defects and a lack of convergent extension are both phenotypes of PCP pathway member mutations (figure 14).

Other members of the Wnt family are known to signal through the Canonical Wnt signaling pathway, otherwise

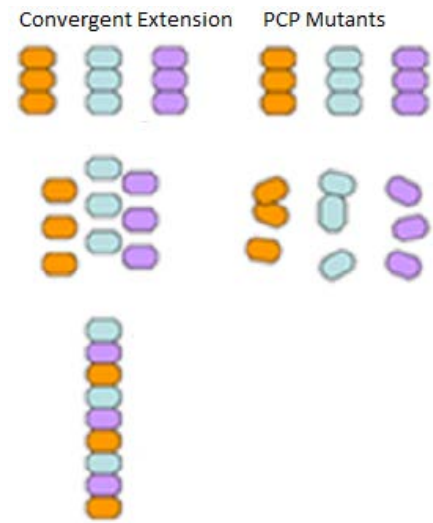


Figure 14: Convergent extension in wild type and PCP mutants

known as the Wnt/ β -catenin pathway. Wnt3a is known to signal through the Wnt/ β -catenin pathway. Wnt3a mutant mice are truncated from the bottom of the ribcage, similar to Wnt5a/Wnt5b mutant mice. It is possible that Wnt5a signals through the Wnt/ β -catenin pathway or through the PCP pathway.

Taken together all these data strongly support Wnt5a signaling through the PCP pathway as a mediator for cell polarity and migration during limb bud development and neural tube closure. Wnt5b, a paralog of Wnt5a, also appears to play a similar role to Wnt5a. Although Wnt5b homozygous mutants are healthy and have no obvious defects, Wnt5a;Wnt5b double mutants have exacerbated phenotypes compared to Wnt5a mutants (figure 15) (Kendall et al. Unpublished).

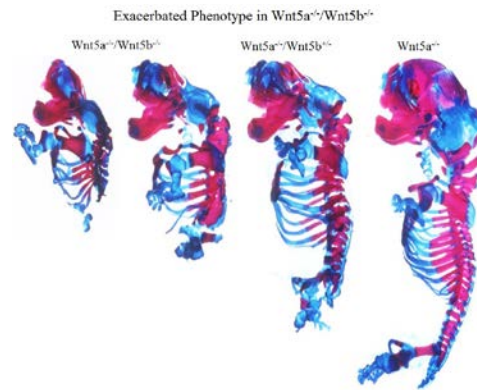


Figure 15: Wnt5a/5b mutant defects (Kendall, Barrott and Barrow Unpublished)

PROPOSAL

Hypothesis

As discussed above, we propose that FGFs signal from the AER induce a Wnt5a in gradient fashion. We also propose that the Wnt5a gradient is necessary and sufficient for directed growth of the mesenchyme toward the highest concentration of Wnt5a. We further propose that Wnt5a and its closely related family member, Wnt5b, play a similar role in regulating the directed movement of cells in the neural plate and notochord which underlies proper neural tube closure.

Objectives and Overview

Specific aim #1: We will test the hypothesis that FGFs expressed in the AER are sufficient to induce a Wnt5a gradient in the distal tip of the limb bud. This Wnt5a gradient is responsible for directed migration of mesenchymal cells of the limb bud toward the distal tip of the limb bud.

FGF4 induction of Wnt5a: We will test the sufficiency of Fgf4 to induce Wnt5a expression in the limb mesenchyme and in the lateral plate mesenchyme. We will transplant beads soaked in varying concentrations of Fgf4 protein into proximal chick embryonic limbs, outside of the expression domain of Wnt5a or in the interlimb lateral plate mesenchyme, and then examine the expression of Wnt5a in nearby mesenchyme. We will window eggs of chick embryos at stages 19-20 and remove the AER. We will place beads that have been soaked in 1000 $\mu\text{g/ml}$ Fgf4 protein near the distal tip of the limb bud. Beads soaked in PBS will be used as negative controls for these experiments. We will allow embryos to develop for 12 hours, and dissect them out of the egg. Wnt5a expression will then be examined by *in situ* hybridization.

Wnt5a induction should be seen in the area near the Fgf4 bead. Wnt5a should be induced

in a larger area surrounding beads soaked in higher concentrations, indicating the increased induction of Wnt5a across the Fgf4 gradient.

Wnt5a induction of directed cell migration: We will test the sufficiency of Wnt5a on directed migration or oriented cell division of limb mesenchyme cells. We will transplant beads soaked in Wnt5a protein into chick embryonic limbs and examine the behavior of neighboring, labeled mesenchyme cells. We will window eggs of chick embryos at stages 19-20. We will place beads that have been soaked in 1000 $\mu\text{g/ml}$ Wnt5a protein. Mesenchyme cells approximately 50-100 μm from the graft will be labeled with DiI. Beads soaked in PBS will be used as negative controls for these experiments. The windowed eggs will be photographed at 4 hour intervals over a 24-48 hour period to examine the growth of the injected cells relative to the source of Wnt5a protein.

If Wnt5a is responsible for directed cell movement and mitoses, then labeled cells near the implanted bead should be seen moving towards the ectopic source of Wnt5a instead of towards the AER.

Specific Aim #2: We will determine whether Wnt5a and Wnt5b signal through the canonical β -catenin or the Wnt/PCP pathway.

Wnt5a signaling through β -catenin pathway: We will examine whether Wnt5a signals through canonical Wnt signaling by examining the expression of Brachyury, a canonical Wnt signaling target, in Wnt5a mouse mutants at E9. Canonical Wnt signaling activity will also be assessed by crossing the Wnt/ β -catenin β -galactosidase reporter transgene (Batgal) into a Wnt5a mutant background. Wnt5a mutants will be compared to E9 wildtype embryos and to Wnt3a mutants

which lack Wnt/ β -catenin signaling in the primitive streak/tailbud and therefore Brachyury and Batgal activity.

If Wnt5a is signaling through the Wnt/ β -catenin signaling, no Brachyury expression or X-gal stain should be seen in the tail of the mouse embryos. These embryos will be compared to wildtype and Wnt3a mutant embryos, which have disrupted Wnt/ β -catenin signaling. We expect that Wnt5a mice will not show disrupted Wnt/ β -catenin signaling, similar to the wildtype embryos.

Convergent extension defects of midline cells in Wnt5a/Wnt5b mutants: We will compare Wnt5a/Wnt5b mutants to Vangl2 mutants for proper convergent extension in the midline at E8.5. We will use *in situ* hybridization for Brachyury mRNA to examine midline cells to see if they have converged on the midline of the embryo properly.

The midlines of E8 Vangl2 mutant mouse embryos express Brachyury mRNA in a broader domain than control mice due to defects in convergent extension. If Wnt5a;Wnt5b mice are signaling through the PCP pathway, then similar defects should be seen.

Length-to-width ratios of Wnt5a/Wnt5b mutants: Vangl2 mutants have previously been reported to exhibit reductions in the length to width (LTW) ratio of the embryonic axis. We predict that if Wnt5a/Wnt5b signal through the Wnt/PCP pathway that these mutants should exhibit a similar reduction in LTW ratio. We will therefore compare the LTW ratio of Wnt5a $-/-$, Wnt5a $-/-$;Wnt5b $+/-$ and Wnt5a/5b double mutants to Vangl^{L^{pt}} mutants.

Vangl2 a known component of the Wnt/PCP pathway and is critical for convergent extension. Mice lacking various components of the PCP pathway exhibit reduction in the length to width ratio of the embryonic axis: a manifestation of defective convergent extension

movements. If Wnt5a/Wnt5b signal via the PCP pathway we predict that embryos lacking their activity should exhibit a reduction in the LTW ratio of the embryonic axis.

Neural tube cell polarity defects: Wnt5a/5b mutants and Vangl^{Lpt} both exhibit neural tube closure defects. We will examine polarity of cells in sections of the neural tube in Wnt5a;Wnt5b and Vangl2^{Lpt} mouse mutants. Coronal and transverse sections of E8.5 mutant and wildtype embryos will be stained for Golgi and nuclei. In normal neural tubes the Golgi apparatus lies between the nucleus and the lumen of the neural tube. We predict that Vangl2 and putatively Wnt5a/5b mutants will exhibit a loss in this polarity. Similar defects between Vangl2 and Wnt5a;Wnt5b mutants provide support for the theory that Wnt5a and Wnt5b are indeed signaling through the PCP pathway.

If Wnt5a and Wnt5b are signaling through the PCP pathway, then defects in cell polarity similar to Vangl^{Lpt} mutants should be seen.

RESULTS

FGF4 induction of Wnt5a expression

The AER is vital for limb bud outgrowth. Our hypothesis is that FGFs from the AER induce a distal Wnt5a gradient in the limb bud. The Wnt5a gradient then directs the migration and cell division of mesenchymal cells in the limb bud toward the AER, causing the limb bud to extend distally.

To determine whether FGF signaling is sufficient to activate Wnt5a expression, Affi-gel blue beads (Bio-Rad) were soaked in 1000 $\mu\text{g}/\mu\text{L}$ FGF4 and implanted in the flank of HH stage 10-12 chick embryos at varying distances from the limb bud. After seven hours of development, Embryos were removed from the egg, fixed in 4% paraformaldehyde (PFA) and then subjected to Wnt5a in situ hybridization.

FGF4 beads induced Wnt5a expression, while control beads did not (figure 16A-F). Beads placed far away from limb buds (figure 16B-C) induced Wnt5a expression in between it and the limb bud, instead of just around the bead, indicating that FGF alone is not sufficient to induce Wnt5a expression. Some other diffusible signal from the

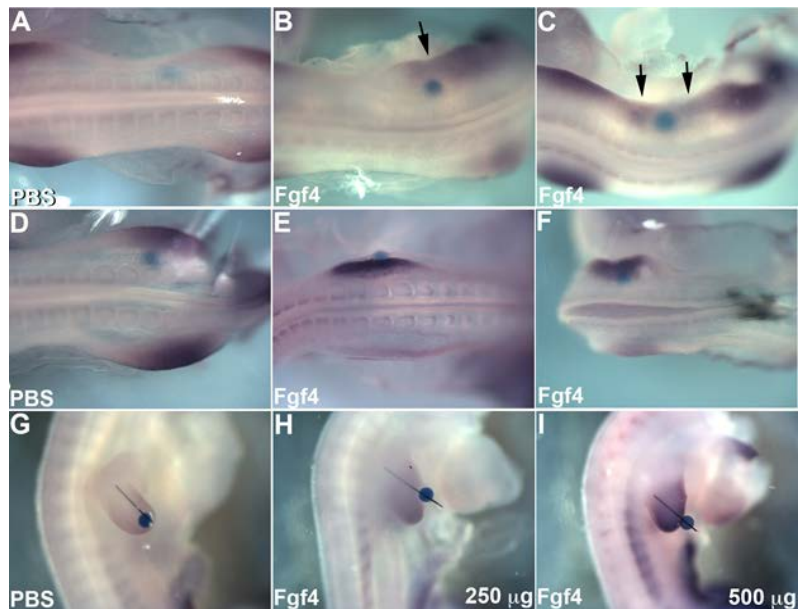


Figure 16: Wnt5a induction in response to varying concentrations of FGF4. FGF4 soaked beads implanted near the limb bud induce strong Wnt5a expression (E, F). Beads implanted in the flank of the embryo induce Wnt5a expression, but only near the limb bud (B, C). FGF4 beads implanted in the distal tip of the limb bud after the AER was removed induce a Wnt5a gradient (H, I).

limb bud is also required. Beads placed in or near the limb bud strongly upregulate Wnt5a expression (figure 16E-F). Affi-gel blue beads soaked in varying concentrations of FGF4 were implanted at the distal tip of HH stage 19-22 chick embryos after the AER was removed. After 12 hours, Wnt5a expression was examined by *in situ* hybridization. Wnt5a expression increased with increasing FGF4 concentration (figure 16G-I).

To determine the ability of Wnt5a to induce directed cell migration, Affi-gel blue beads were soaked in Wnt5a protein and implanted in the limb buds of HH stage 19-22 chick embryos. DiI

was injected anteriorly and posteriorly of the implanted bead and pictures were taken at 4 hour intervals. Cells as visualized by DiI labeling migrated toward the

Wnt5a soaked bead instead of the AER (figure 17B, C), compared with control beads, which

displayed no apparent cell migration toward the bead, only toward the AER (figure 17A).

displayed no apparent cell migration toward the bead, only toward the AER (figure 17A).

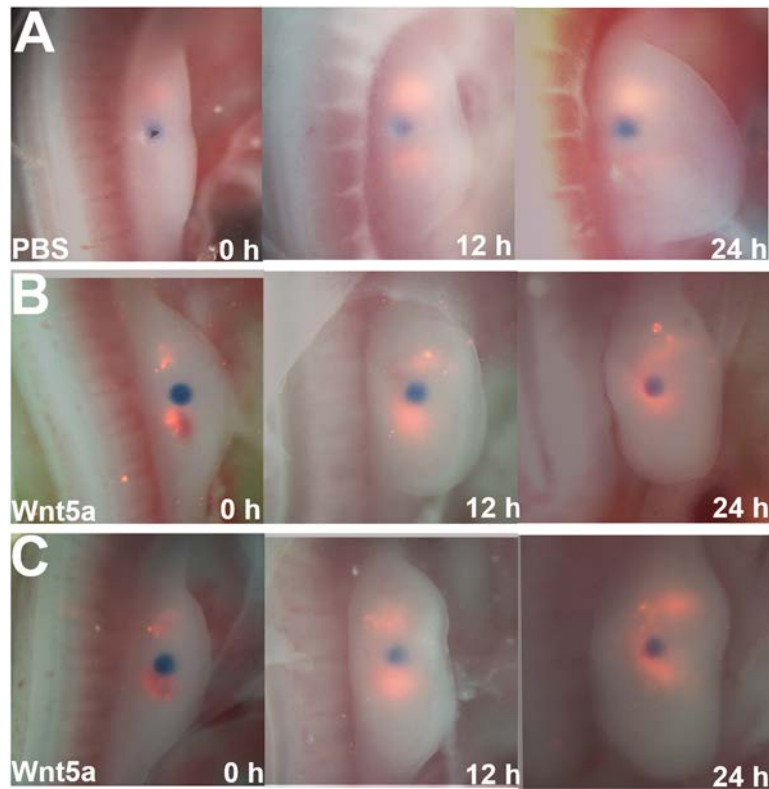


Figure 17: Directed mesenchymal cell migration in response to Wnt5a

Wnt5a signaling through the PCP pathway

Wnt5a and Wnt5a/Wnt5b mutants share defects in common with mice lacking components of the Wnt/ β -catenin and the Wnt/PCP pathway. For example, Wnt3a is a secreted

Wnt ligand that is known to signal through the β -catenin pathway (Ring et al. 2013). Mouse embryos lacking Wnt3 are truncated to the rig cage (Takada et al. 1994) similar to Wnt5a/Wnt5b mutants (figure 16) suggesting that Wnt5a/Wnt5b signal through the β -catenin pathway. Wnt5a mutants also exhibit neural tube closure defects, shortening of the body axis, face, limbs similar to mutants lacking components of the PCP pathway. To determine the pathway through which Wnt5a and Wnt5b signal we performed several genetic analyses.

Wnt3a as mentioned above signals through the β -catenin pathway but not the PCP pathway. We made use of the transgenic mouse model Batgal that reports β -galactosidase

activity in cells actively receiving a Wnt/ β -catenin signal (Maretto et al. 2003). We observed as expected reduced β -galactosidase activity in the primitive streak/tail bud of Wnt3a mutant embryos (figure 18C). In contrast we observed no reduction in batgal activity in the primitive streak of Wnt5a mutants providing strong evidence that Wnt5a signals independently of the β -catenin pathway (figure 18B).

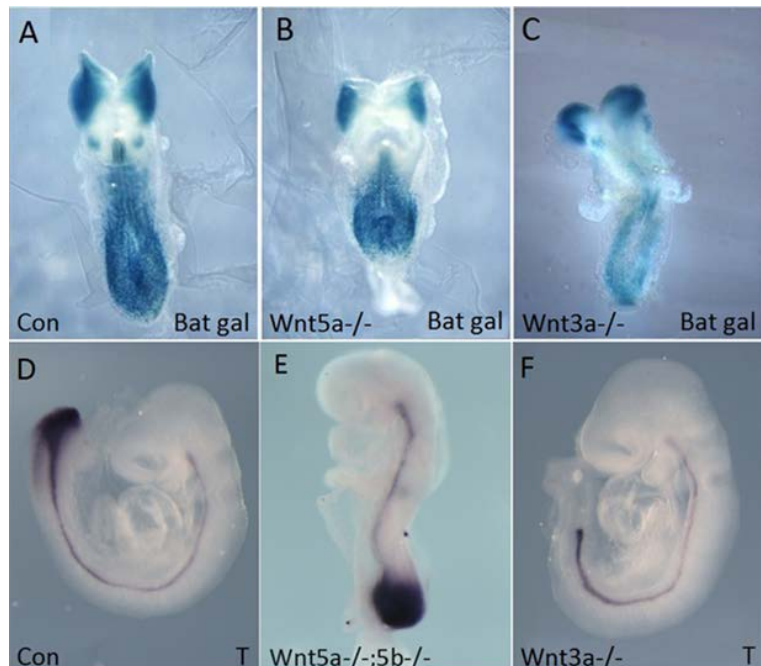


Figure 18: Wnt5a/Wnt5b mutants maintain β -catenin signaling while Wnt3a mutants do not

Wnt5a/Wnt5b double mutants exhibit more severe axis truncation defects than Wnt5a single mutants (similar to Wnt3a mutants). It is possible that the two function redundantly in the β -catenin pathway. To test this hypothesis we examined the expression of the Wnt/ β -catenin

target, Brachyury (Yamaguchi et al. 1999b). We observed strong Brachyury expression in the tailbud of Wnt5a/5b double mutants (figure 18E) and loss thereof in Wnt3a mutants (figure 18F). Thus, taken together the Batgal and the brachyury results demonstrate that Wnt5a and Wnt5b signal via a β -catenin independent pathway

We next wanted to test that hypothesis that Wnt5a and Wnt5b signal through the PCP pathway. Vangl2 is a well characterized member of the Wnt/Planar Cell Polarity pathway. It is a 4 pass membrane protein of poorly understood function. We postulated that if Wnt5a and Wnt5b signal via the PCP pathway that Wnt5a/Wnt5b mutants should closely resemble embryos lacking Vangl2. We first examined convergence and extension of the embryonic axis in Wnt5a/Wnt5b mutants and compared them to Vangl2 mutants. Cells of the notochord that undergo convergent extension, the process of cell intercalation and extension, express brachyury. To compare CE defects in Wnt5a/Wnt5b and Vangl2 mutants, brachyury expression was

examined in E8 mutant mice.

Because embryonic development at this stage is very dynamic, embryos were divided into early and late E8 embryos (early E7.8-E8.0 late E8.2-E8.4). Early control E8 embryos have a diffuse region of brachyury expressing cells along the midline, but these

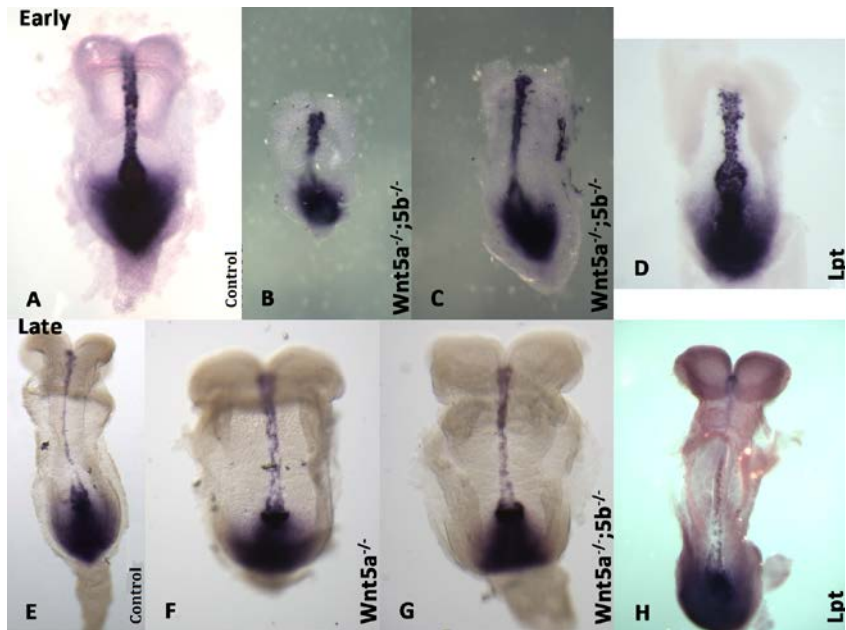


Figure 19: Wnt5a/Wnt5b and Vangl2 (looptail) mutants have similar CE defects in notochord cells. Magnifications are different between specimens.

cells are still confined to a narrow zone, with no gaps or areas with cells that are not expressing brachyury (figure 19A). Wnt5a/Wnt5b mutant midline cells are not strictly confined to the midline, with many brachyury expressing cells outside of the main expression zone (figure 19B-C). The node also fails to retract posteriorly to the extent observed in controls (you will want to label your figures to highlight this observation). Looptail embryos exhibit similar defects (figure 19D). Notochord cells of late E8 wildtype embryos have a single, thin line of brachyury expressing cells that have converged on the midline (figure 19E). Late Wnt5a and Wnt5b mutants possess axial mesoderm cells that exhibit a “crankshaft” appearance with distinct gaps between Brachyury expressing and nonexpressing cells (figure 19G, H). Further, the midline cells do not converge along the midline as do controls (figure 19G, H). These defects are analogous to those observed in *Vangl2*^{L^{pt}} mutants (figure 19H).

As an alternative means to examine convergence and extension, we measured the length to width ratio of the embryonic axis (see Materials and Methods). Next, we examined convergent extension defects in embryonic axis elongation. Briefly, we collected embryos at the 6 somite stage for the Wnt5a/Wnt5b allelic series-and compared to *Vangl2*^{L^{pt}} and wildtype mouse embryos (figure

20). As more Wnt5a/Wnt5b alleles are lost, the embryo becomes shorter. Looptail mutants also exhibit axis elongation defects, but

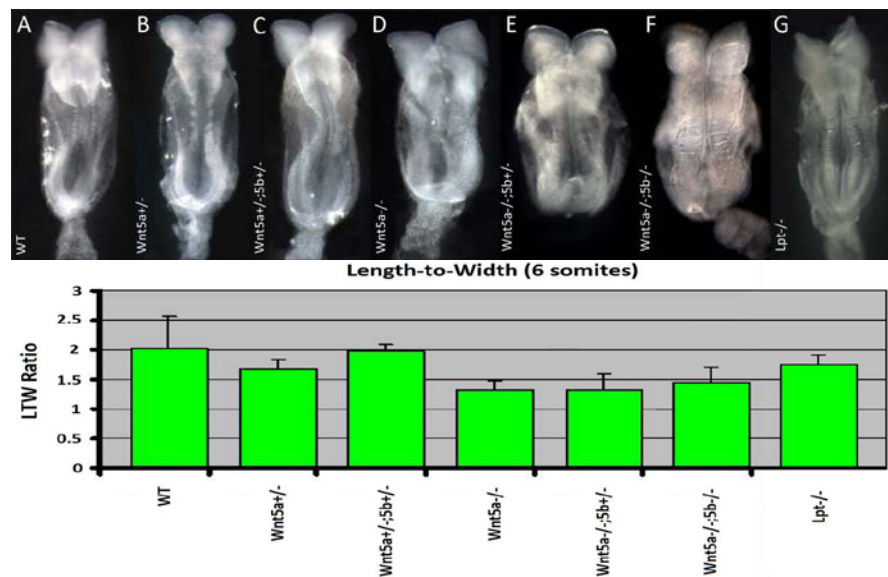


Figure 20: Length to width ratios of various Wnt5a/Wnt5b and looptail genotypes

their severity is reduced. In some cases, losing a Wnt5b allele actually lessens the axis elongation defect.

Next, neural tube defects were examined (Table 1). Partial or complete open neural tube defects were counted as a neural tube defect. Looptail homozygous mutants have 100%

penetrance for open neural tube defects. Approximately 42% of Wnt5a homozygous mutants have neural tube defects. Nearly twice that many defects are seen in Wnt5a/Wnt5b homozygous mutants.

Table 1: Neural tube defects in Wnt5a/Wnt5b and looptail mutants

Mutation	% NTD
Wnt5a ^{-/-} ; 5b ^{+/+}	42%
Wnt5a ^{-/-} ; 5b ^{+/-}	50%
Wnt5a ^{-/-} ; 5b ^{-/-}	82%
Looptail	100%

We theorized that cells of the neural tube undergo convergent extension to bring the halves of the neural tube together for neural tube closure. E8.5 Wnt5a/Wnt5b and looptail mutant mouse embryo hindbrains were sectioned into 150 μm sections. Golgi apparatus and nucleus stain was used to visualize cell orientation. However, no differences between wildtype, Wnt5a/Wnt5b, and looptail embryos have yet been determined.

DISCUSSION

John Saunders demonstrated that the AER directs limb development and patterning and that the signal from the AER does not change over time. Several models have been developed that attempt to describe how the AER patterns the mesenchymal cells of the limb bud, but none of them account for all the data. Our model of limb development, the limb mesenchyme recruitment model, proposes that the shape of the AER dictates the pattern of development in the limb mesenchyme by directing migration of cells towards it. As the AER becomes elongated along the anterior-posterior axis and thinner along the ventral-dorsal axis, the shape of the mesenchyme becomes less round-shaped like the stylopod and more paddle shaped, like the autopod.

We hypothesize that the AER secretes a signal that activates directed migration toward the distal end of the limb bud. We demonstrate that FGF4 from the AER activates a distal gradient of Wnt5a expression in the limb. We have described in this thesis that when FGF4 soaked beads are implanted into the flank of HH stage 10-12 chick embryos induce Wnt5a expression in the limb bud. When the FGF4 bead is implanted closer to the limb bud, endogenous Wnt5a is expressed more strongly, indicating that elevated levels of Wnt5a are expressed with increasing Fgf4 concentration.

We corroborated this observation by demonstrating that beads soaked in higher concentrations of FGF4 maintained Wnt5a expression at higher levels than beads soaked in lower concentrations of FGF4. Taken together these data argue that FGF is sufficient to induce/maintain Wnt5a expression in gradient fashion. A gradient of Wnt5a is likely critical for polarizing limb mesenchyme cells as demonstrated by Goa et al (Gao et al. 2011). As Wnt5a concentration increases, more serines and threonines on Vangl2 are phosphorylated. If a cell is

exposed to a Wnt5a gradient, then Vangl2 is going to be more phosphorylated on the side of the cell that is exposed to a higher concentration of Wnt5a.

We theorized that higher Wnt5a concentrations nearer to the AER induced more rapid cell migration and division in the area near the AER called the zone of polarizing activity (ZPA). Beads soaked in Wnt5a were implanted in the center of stage 19-22 chick embryo limb buds. Using Dil to visualize cell movement, we observed mesenchymal cells migrating toward Wnt5a soaked beads instead of the AER. PBS soaked control beads still migrated distally to the AER. Cells migrated more quickly as they moved closer to the Wnt5a bead, indicating that higher concentrations of Wnt5a cause mesenchymal cells to migrate more rapidly. This supports the theory that the Wnt5a gradient near the AER causes more rapid cell migration and division, which supports the theory that the shape of the AER, and not the signal secreted by it, patterns the limb bud by shaping the mesenchymal cells into a specific shape.

We theorized that Wnt5a induces direction cell migration and division by activating the planar cell polarity pathway in mesenchymal cells of the limb bud. Naturally occurring Vangl2 mutants, known as looptail mice were used to compare Vangl2 mutations to Wnt5a and Wnt5b mutations to determine if similar phenotypes were seen. If Wnt5a signals through the PCP pathway, then similar defects should be seen.

Many Wnts signal through the canonical β -catenin signaling pathway. To demonstrate that Wnt5a signals through the PCP pathway and not the β -catenin pathway, we compared Wnt3a, which is known to signal through the β -catenin pathway, to Wnt5a and Wnt5b. β -galactosidase was used as a reporter gene for β -catenin signaling activity. When β -catenin is active, β -galactosidase is expressed, which cleaves X-gal into a product that is blue. Wnt3a mutants embryos did not maintain β -catenin activity, while Wnt5a mutants did. Brachyury in the tail bud

is a target gene of the β -catenin pathway. Similarly, Wnt3a mutants lost brachyury expression in the tail bud while Wnt5a mutants and Wnt5a;Wnt5b double mutants did not. These results indicate that Wnt5a and Wnt5b do not signal through the β -catenin signaling pathway.

To demonstrate that Wnt5a and Wnt5b signal through the PCP pathway, mutants were compared to Vangl^{L^{pt}} mutant mice, which have a mutation in Vangl2, a component of the PCP pathway. Activation of the PCP pathway polarizes cells within tissues. Once polarized, cells can grow directionally. A topic of debate within the PCP field has been to determine the nature of the signals that regulate the PCP pathway to initiate polarity. This thesis work provides important data to establish Wnt5a and Wnt5b as signals that regulate the Wnt/PCP pathway.

Reintroduce the theory behind using Vangl2 mutants as a comparison to Wnt5a/Wnt5b mutants. First, we examined convergent extension defects in early and late E8 mouse embryos. At E8, cells of the notochord undergo convergent extension causing the entire embryo to become thinner and longer. Defects in CE can be seen by staining for brachyury, which is expressed by cells of the notochord. Early E8 embryos have a single line of brachyury expressing cells along the notochord. Wnt5a/Wnt5b mutants at this stage have a line of cells along the notochord, but they are not lined up neatly like control embryos, instead the notochord cells are not restricted to the cells of the midline. Vangl2 mutants have a similar appearance. PCP in these cells is at least partially disrupted, so cells do not converge entirely on the midline of the embryo. Wnt5a/Wnt5b embryos and Vangl2 embryos have a nearly similar appearance, indicating an at least partial loss of PCP signaling.

In late E8 embryos, notochord cells continue to converge on the midline of the embryo. The entire embryo is longer and thinner and the brachyury expression domain is thinner. In Wnt5a mutants, notochord cells have a “crankshaft” appearance, with gaps in brachyury

expression that alternates sides. Wnt5a/Wnt5b mutants look similar, with gaps in brachyury expression. Vangl2 mutants display a similar phenotype, with breaks in the brachyury expression zone, further indicating a similar loss in PCP signaling.

Next, we examined convergent and extension defects in the entire embryo. Length and width measurements were taken in Vangl2 and various combinations of Wnt5a/Wnt5b mutant alleles. Length to width ratios were shorter for Wnt5a/Wnt5b double mutants compared to Vangl2 mutants. As either Wnt5a or Wnt5b alleles were lost, embryos became progressively shorter. Interestingly, some Wnt5b mutations actually abrogated Wnt5a mutations, causing the embryo to be slightly longer than expected. We do not have an explanation for why this occurs. It is possible that Wnt5b somehow mediates the effects of Wnt5a. Function of Wnt5b beyond PCP pathway activation is outside of the scope of this thesis.

Additionally, we examined neural tube defects in Vangl2 and Wnt5a/Wnt5b mutants. All Vangl2 mutants had open neural tube defects. Additionally, neural tube defects in these mutants were more severe, extending from the hindbrain to the tail bud. Only 42% of Wnt5a^{-/-} mutants had neural tube defects, which ranged in severity from being open near the hindbrain to extending further along the embryonic axis. Neural tube defects in Wnt5a^{-/-}/Wnt5b^{+/-} mutants grew to 50% and 82% of Wnt5a^{-/-}/Wnt5b^{-/-} embryos.

It is worth noting that Wnt5a and Wnt5b mutations result in more severe axis elongation defects, while Vangl2 mutations result in more severe neural tube defects. There are 19 members of the Wnt protein family. It is possible that other Wnts are also responsible for activating the PCP pathway in the neural tube. It is also possible that Vangl1, a homolog to Vangl2 with a similar role in PCP signaling, could be partially responsible for convergent extension of the embryonic axis, while only Vangl2 is responsible for convergent extension in

neural tube closure. Previous studies examine the role of Ror2 as a receptor for Wnt5a in mesenchymal cell migration (Barrow et al. 2010). Other members of the Ror receptor family include Ror1 and Ryk (Katoh 2005, Andre et al. 2012). These receptors have not been examined for a role in PCP signaling, and so it is possible that different receptors have different temporal or spatial roles in the developing embryo.

Last of all, we examined cell behavior in the neural tube during neural tube closure. We sectioned E8.5 mouse embryo hindbrains and stained for nucleus and Golgi apparatus. We examined these cells for differences in cell division and migration, but could see no major differences. Again, not all $Wnt5a^{-/-}/Wnt5b^{-/-}$ mutants had neural tube defects. It's possible that other Wnts mitigate the loss of Wnt5a and Wnt5b, or that Wnt5a and Wnt5b only have a minor role in neural tube closure.

METHODS

Windowing eggs

Eggs are incubated until they reach HH stage 20 (Hamburger and Hamilton 1992), sprayed with isopropanol and, the top of the egg is covered in two strips of Scotch® Super 33+ Vinyl Electrical Tape. 8 mL of albumin is removed using an 18 ga 1.5 in needle (Becton Dickinson) and a hole is cut into the top of the egg. Five drops of penicillin-streptomycin-glutamaine (PSG) in phosphate buffered saline (PBS) are added to prevent dehydration and bacterial growth. A 25 ga 1.5 in needle (Becton Dickinson) is used to inject a 1:10 India ink (Pelikan Fount India) with Dulbecco's PBS (GIBCO) under the embryo for easier visualization. The eggs are then sealed with electrical tape until beads are implanted.

Wnt5a Bead Implants

We will window chicken eggs and inject India ink under the embryo. We will introduce an ectopic source of Wnt5a protein outside of the distal limb bud where Wnt5a is normally expressed by implanting a bead soaked in Wnt5a protein in the proximal limb bud. We will label the cells anterior and posterior to the implanted beads with Dil. We will photograph these embryos every 4 hours for 24-48 hours.

FGF Bead Implants

We will introduce an ectopic source of Fgf4 protein in the distal limb bud by implanting a bead soaked in Fgf4 protein. We will remove the AER using a tungsten wire and implant the bead near the distal tip of the limb bud. To reproduce the effects of an Fgf4 gradient, we will soak the beads in differing concentrations of Fgf4. These embryos will continue to develop for twelve hours. We will then dissect the embryos from the eggs and examine Wnt5a expression by

in situ hybridization.

Mouse Strains and Genotyping

Mice carrying Wnt5a mutation were obtained from Andy McMahon's lab at Harvard University and genotyped using the following set of primers: 5a neo (5'-GGG AGC CGG TTG GCG CTA CCG GTG G), wnt5a-for (5'-GAC TTC CTG GTG AGG GTG CGT G), wnt5a-rev (5'-GGAGAA TGG GCA CAC AGA ATC AAC). The following reaction for PCR was used: 94 °C for 30 seconds, 55 °C for 20 seconds, 72 °C for 30 seconds; 35 cycles.

in situ Hybridization

Embryos were fixed in 4% paraformaldehyde and processed for in situ hybridization. Preparation of digoxigenin-labeled probes was carried out according to the manufacturer's protocol (Roche). Embryos were collected in PBS, fixed in 4% paraformaldehyde overnight, dehydrated, and stored in 100% methanol. After rehydrating embryos through a 75, 50, and 25% methanol series, embryos were bleached with a 4:1 mixture of PBT and 30% hydrogen peroxide. Embryos were incubated with 20 µg/ml of proteinase K for 2 min for E8 embryos and 5 min for E9 embryos and washed twice with fresh 2 mg/ml glycine, washed twice with PBT, refixed in 4% paraformaldehyde and 0.2% glutaraldehyde for 20 min, and incubated in pre-hybridization solution (50% formamide, 5X SSC pH 4.5, 1% SDS, autoclave H₂O, 50 µg/ml tRNA, 50 µg/ml heparin) at 68°C for 1 hour. Embryos were incubated in hybridization solution (pre-hybridization + 5 µl/ml brachyury probe) overnight at 68°C. The next day, embryos were washed twice with solution I (50% formamide, autoclave H₂O, 5X SSC pH 4.5, and 1% SDS) at 68 °C for 30 minutes, then equilibrated for 10 minutes in a 1:1 mix of solutions I and II at 68 °C. Embryos were washed three times in solution II (10% 5M NaCl, 1% 1M Tris-HCl pH 7.5,

0.1% tween-20, and autoclave H₂O) at RT. Embryos were then treated with 100 µg/ml RNaseA in solution II for 1 hour at 37 °C, and subsequently washed in solution II for 5 minutes at RT. Embryos were washed twice in solution III (50% formamide, 2X SSC pH 4.5, and autoclave H₂O) for 30 minutes at 68 °C. Then the embryos were washed three times in MBST and then place in a preblock solution (10% heat-inactivated sheep serum) for 2.5 hours at RT, embryos were treated with a 1:5000 dilution of anti-digoxigenin Fab fragments (Roche) overnight at 4 °C. After thorough washing with NTMT (2% 5M NaCl, 10% 1M Tris-HCl pH 9.5, 1M MgCl₂, 0.1% tween-20, and autoclave H₂O), the hybridization products were visualized using BM purple (Roche) as a substrate. The following probes were used in the in situ expression studies: Brachyury, Wnt5a, Wnt3a.

X-gal Staining

Embryos are washed 3x with PBS and then fixed at room temperature in pre-fixative (1% formaldehyde, 0.2% glutaraldehyde, 2 mM MgCl₂, 5 mM EGTA, 0.02% NP-40 in PBS) for 30-60 min. Embryos are washed 3x in PBS and stained in X-gal solution (5 mM K₃Fe(CN)₆, 5 mM K₄Fe(CN)₆, 2 mM MgCl₂, 0.01% NaDeoxycholate, 0.02% NP-40, 1 mg/mL X-gal) until target areas are blue, but before embryos are overstained. Embryos are washed 3x in PBS and fixed in PFA overnight. Embryos are stored in 80% glycerol in PBS.

Length-to-Width Ratio (LWR) Measurement in Neurulating Embryos

Embryos derived from appropriate crosses were dissected at E8.5, presence of a seminal plug the following morning marked E0.5. Yolk sacs were removed for PCR genotyping. Embryos were fixed and stored in 4% paraformaldehyde at 4°C. Before fixing in paraformaldehyde, embryos were transferred to an empty dish and allowed to extend naturally.

After counting somite numbers, embryos were photographed with an Olympus U-CMAD3 camera mounted on an Olympus SZX12 dissection microscope. Images of the dorsal view of each embryo were acquired and imported into Adobe Photoshop 7.0 and length-to-width measurements of the trunk of the embryo were made as follows. On each embryo, a two lines were drawn from the base of the left and right side of the headfold to the base of the allantois. The average of these two lines was used for the length measurement. The width measurement was obtained by drawing at least three lines posterior to the headfold from one lateral side to the other lateral side and averaging the measurements of the total number of widths taken. A total of 170 embryos were taken and measured and statistical analysis was performed by using the Kruskal-Wallis test, non-parametric ANOVA test.

Embryo Collection, Embedding, and Sectioning

Embryos are dissected into PBS, straightened in 4% paraformaldehyde (PFA), and then fixed in 4% PFA at least for 24 hours. Embryos are washed 3x in PBS and then embedded headfold down in 15% gelatin in PBS in a mold. The gelatin is allowed to harden overnight in a slide box with a wet paper towel. A razor is used to cut the mold and excess gelatin off, leaving a small block of gelatin containing the embryo. The gelatin is fixed in PFA overnight. The block is then sectioned into 150 μm sections using a vibratome sectioner.

Immunohistochemistry

Primary antibody (Golgi (GM130)) are added to a 0.1% tween and 0.1% BSA in PBS solution at a 1:100 concentration. 125 μL of antibody solution is added to each section and allowed to incubate at 4 $^{\circ}\text{C}$ overnight. The sections are washed and nutated 3x with PBS for 5 min. 125 μL of secondary antibody (Mouse IgG K Alexa 488) is then added to each section at a

1:500 concentration in a 0.1% tween and 0.1% BSA in PBS and incubated for 1 hour at room temperature. The sections are washed and nutated 3x with PBS for 5 min. 125 μ L of To-pro diluted 1:250 in 0.1% tween and 0.1% BSA in PBS is added to each section and incubated for 10 min at room temperature. The sections are washed and nutated 3x with PBS for 5 min. The sections are transferred to a microscope slide, sealed under a coverslip using vectashield and nail polish around the edges. Slides are stored for up to 7 days at 4 °C and confocal images are taken.

WORKS CITED

- Andre, P., Q. Wang, N. Wang, B. Gao, A. Schilit, M. M. Halford, S. A. Stacker, X. Zhang & Y. Yang (2012) The Wnt coreceptor Ryk regulates Wnt/planar cell polarity by modulating the degradation of the core planar cell polarity component Vangl2. *Journal of Biological Chemistry*.
- Antic, D., J. L. Stubbs, K. Suyama, C. Kintner, M. P. Scott & J. D. Axelrod (2010) Planar Cell Polarity Enables Posterior Localization of Nodal Cilia and Left-Right Axis Determination during Mouse and Xenopus Embryogenesis. *PLoS One*, 5, e8999.
- Barrow, J. R. (2006) Wnt/PCP signaling: A veritable polar star in establishing patterns of polarity in embryonic tissues. *Seminars in Cell & Developmental Biology*, 17, 185-193.
- Barrow, J. R. (Unpublished).
- Barrow, J. R., T. M. Dahl, A. P. Smith, K. E. Kmetzsch, J. J. Barrott, J. J. Kendall & K. L. Low (2010) The Limb Mesenchyme Recruitment Model for Patterning the Vertebrate Limb. *Developmental Biology*, 344, 444-445.
- Barrow, J. R. p., K. R. p. Thomas, O. p. Boussadia-Zahui, R. p. Moore, R. p. Kemler, M. R. p. Capecchi & A. P. p. McMahon (2003) Ectodermal Wnt3/beta-catenin signaling is required for the establishment and maintenance of the apical ectodermal ridge. *Genes Dev*, 17, 394-409.
- Boulet, A. M., A. M. Moon, B. R. Arenkiel & M. R. Capecchi (2004) The roles of Fgf4 and Fgf8 in limb bud initiation and outgrowth. *Developmental Biology*, 273, 361-372.
- Cohn, M. J., J. C. Izpisua-Belmonte, H. Abud, J. K. Heath & C. Tickle (1995) Fibroblast growth factors induce additional limb development from the flank of chick embryos. *Cell*, 80, 739-746.
- Copp, A. J., N. D. E. Greene & J. N. Murdoch (2003) Dishevelled: linking convergent extension with neural tube closure. *Trends in Neurosciences*, 26, 453-455.
- Crossley, P. H. & G. R. Martin (1995) The mouse Fgf8 gene encodes a family of polypeptides and is expressed in regions that direct outgrowth and patterning in the developing embryo. *Development*, 121, 439-451.
- Doudney, K. & P. Stanier (2005) Epithelial cell polarity genes are required for neural tube closure. *American Journal of Medical Genetics Part C: Seminars in Medical Genetics*, 135C, 42-47.
- Dudley, A. T., M. A. Ros & C. J. Tabin (2002) A re-examination of proximodistal patterning during vertebrate limb development. *Nature*, 418, 539-544.
- Fallon, J., A. Lopez, M. Ros, M. Savage, B. Olwin & B. Simandl (1994) FGF-2: apical

- ectodermal ridge growth signal for chick limb development. *Science*, 264, 104-107.
- Gao, B., H. Song, K. Bishop, G. Elliot, L. Garrett, M. A. English, P. Andre, J. Robinson, R. Sood, Y. Minami, A. N. Economides & Y. Yang (2011) Wnt Signaling Gradients Establish Planar Cell Polarity by Inducing Vangl2 Phosphorylation through Ror2. *Developmental cell*, 20, 163-176.
- Gong, Y., C. Mo & S. E. Fraser (2004) Planar cell polarity signalling controls cell division orientation during zebrafish gastrulation. *Nature*, 430, 689-693.
- Gros, J., J. K.-H. Hu, C. Vinegoni, P. F. Feruglio, R. Weissleder & C. J. Tabin (2010) WNT5A/JNK and FGF/MAPK Pathways Regulate the Cellular Events Shaping the Vertebrate Limb Bud. *Current biology : CB*, 20, 1993-2002.
- Hamburger, V. & H. L. Hamilton (1951) A series of normal stages in the development of the chick embryo. 1951. *Dev Dyn*, 195, 231-72.
- He, F., W. Xiong, X. Yu, R. Espinoza-Lewis, C. Liu, S. Gu, M. Nishita, K. Suzuki, G. Yamada, Y. Minami & Y. Chen (2008) Wnt5a regulates directional cell migration and cell proliferation via Ror2-mediated noncanonical pathway in mammalian palate development. *Development*, 135, 3871-3879.
- Heisenberg, C.-P., M. Tada, G.-J. Rauch, L. Saude, M. L. Concha, R. Geisler, D. L. Stemple, J. C. Smith & S. W. Wilson (2000) Silberblick/Wnt11 mediates convergent extension movements during zebrafish gastrulation. *Nature*, 405, 76-81.
- Jones, C. & P. Chen (2007) Planar cell polarity signaling in vertebrates. *BioEssays*, 29, 120-132.
- Katoh, M. (2005) Comparative genomics on ROR1 and ROR2 orthologs. *Oncol Rep*, 14, 1381-4.
- Kawakami, Y., N. Wada, S.-i. Nishimatsu, T. Ishikawa, S. Noji & T. Nohno (1999) Involvement of Wnt-5a in chondrogenic pattern formation in the chick limb bud. *Development, Growth & Differentiation*, 41, 29-40.
- Kendall, J. J., J. J. Barrott & J. R. Barrow (Unpublished).
- Kibar, Z., E. Torban, J. R. McDearmid, A. Reynolds, J. Berghout, M. Mathieu, I. Kirillova, P. De Marco, E. Merello, J. M. Hayes, J. B. Wallingford, P. Drapeau, V. Capra & P. Gros (2007) Mutations in VANGL1 Associated with Neural-Tube Defects. *New England Journal of Medicine*, 356, 1432-1437.
- Kilian, B., H. Mansukoski, F. C. Barbosa, F. Ulrich, M. Tada & C.-P. Heisenberg (2003) The role of Ppt/Wnt5 in regulating cell shape and movement during zebrafish gastrulation. *Mechanisms of Development*, 120, 467-476.
- Lewandoski, M., X. Sun & G. R. Martin (2000) Fgf8 signalling from the AER is essential for normal limb development. *Nat Genet*, 26, 460-3.

- Li, S. & K. Muneoka (1999) Cell Migration and Chick Limb Development: Chemotactic Action of FGF-4 and the AER. *Developmental Biology*, 211, 335-347.
- Litingtung, Y., R. D. Dahn, Y. Li, J. F. Fallon & C. Chiang (2002) Shh and Gli3 are dispensable for limb skeleton formation but regulate digit number and identity. *Nature*, 418, 979-83.
- Macheda, M. L., W. W. Sun, K. Kugathasan, B. M. Hogan, N. I. Bower, M. M. Halford, Y. F. Zhang, B. E. Jacques, G. J. Lieschke, A. Dabdoub & S. A. Stacker (2012) The Wnt Receptor Ryk Plays a Role in Mammalian Planar Cell Polarity Signaling. *Journal of Biological Chemistry*, 287, 29312-29323.
- Mao, J., J. Barrow, J. McMahon, J. Vaughan & A. P. McMahon (2005) An ES cell system for rapid, spatial and temporal analysis of gene function in vitro and in vivo. *Nucleic Acids Research*, 33, e155.
- Maretto, S., M. Cordenonsi, S. Dupont, P. Braghetta, V. Broccoli, A. B. Hassan, D. Volpin, G. M. Bressan & S. Piccolo (2003) Mapping Wnt/ β -catenin signaling during mouse development and in colorectal tumors. *Proceedings of the National Academy of Sciences*, 100, 3299-3304.
- Mariani, F. V. & G. R. Martin (2003) Deciphering skeletal patterning: clues from the limb. *Nature*, 423, 319-325.
- Montcouquiol, M., E. B. Crenshaw & M. W. Kelley (2006a) Noncanonical Wnt signaling and neural polarity. *Annual Review of Neuroscience*, 29, 363-386.
- Montcouquiol, M., N. Sans, D. Huss, J. Kach, J. D. Dickman, A. Forge, R. A. Rachel, N. G. Copeland, N. A. Jenkins, D. Bogani, J. Murdoch, M. E. Warchol, R. J. Wenthold & M. W. Kelley (2006b) Asymmetric localization of Vangl2 and Fz3 indicate novel mechanisms for planar cell polarity in mammals. *J Neurosci*, 26, 5265-75.
- Moon, A. M. & M. R. Capecchi (2000) Fgf8 is required for outgrowth and patterning of the limbs. *Nat Genet*, 26, 455-9.
- Niswander, L. & G. R. Martin (1992) Fgf-4 expression during gastrulation, myogenesis, limb and tooth development in the mouse. *Development*, 114, 755-68.
- Niswander, L., C. Tickle, A. Vogel, I. Booth & G. R. Martin (1993) FGF-4 replaces the apical ectodermal ridge and directs outgrowth and patterning of the limb. *Cell*, 75, 579-587.
- Qian, D., C. Jones, A. Rzadzinska, S. Mark, X. Zhang, K. P. Steel, X. Dai & P. Chen (2007) Wnt5a functions in planar cell polarity regulation in mice. *Developmental Biology*, 306, 121-133.
- Rauch, G. J., M. Hammerschmidt, P. Blader, H. E. Schauerte, U. Strahle, P. W. Ingham, A. P. McMahon & P. Haffter (1997) Wnt5 is required for tail formation in the zebrafish embryo. *Cold Spring Harb Symp Quant Biol*, 62, 227-34.

- Ring, L., P. Neth, C. Weber, S. Steffens & A. Faussner (2013) beta-Catenin-dependent pathway activation by both promiscuous "canonical" WNT3a-, and specific "noncanonical" WNT4- and WNT5a-FZD receptor combinations with strong differences in LRP5 and LRP6 dependency. *Cell Signal*, 26, 260-267.
- Rubin, L. & J. W. Saunders (1972) Ectodermal-mesodermal interactions in the growth of limb buds in the chick embryo: Constancy and temporal limits of the ectodermal induction. *Developmental Biology*, 28, 94-112.
- Sakaguchi, S., Y. Nakatani, N. Takamatsu, H. Hori, A. Kawakami, K. Inohaya & A. Kudo (2006) Medaka unextended-fin mutants suggest a role for Hoxb8a in cell migration and osteoblast differentiation during appendage formation. *Developmental Biology*, 293, 426-438.
- Saunders, J. W., Jr. (1948) The proximo-distal sequence of origin of the parts of the chick wing and the role of the ectoderm. *J Exp Zool*, 108, 363-403.
- Saxton, T. M., B. G. Ciruna, D. Holmyard, S. Kulkarni, K. Harpal, J. Rossant & T. Pawson (2000) The SH2 tyrosine phosphatase Shp2 is required for mammalian limb development. *Nat Genet*, 24, 420-423.
- Sowby, W. H. & J. R. Barrow (Unpublished).
- Summerbell, D. & J. H. Lewis (1975) Time, place and positional value in the chick limb-bud. *Journal of Embryology and Experimental Morphology*, 33, 621-643.
- Summerbell, D., J. H. Lewis & L. Wolpert (1973) Positional information in chick limb morphogenesis. *Nature*, 244, 492-6.
- Sun, X., F. V. Mariani & G. R. Martin (2002) Functions of FGF signalling from the apical ectodermal ridge in limb development. *Nature*, 418, 501-508.
- Tabin, C. & L. Wolpert (2007) Rethinking the proximodistal axis of the vertebrate limb in the molecular era. *Genes Dev*, 21, 1433-42.
- Takada, S., K. L. Stark, M. J. Shea, G. Vassileva, J. A. McMahon & A. P. McMahon (1994) Wnt-3a regulates somite and tailbud formation in the mouse embryo. *Genes Dev*, 8, 174-89.
- Ueno, N. & N. D. E. Greene (2003) Planar cell polarity genes and neural tube closure. *Birth Defects Research Part C: Embryo Today: Reviews*, 69, 318-324.
- Vargesson, N., J. D. Clarke, K. Vincent, C. Coles, L. Wolpert & C. Tickle (1997) Cell fate in the chick limb bud and relationship to gene expression. *Development*, 124, 1909-1918.
- Wallingford, J. B. (2006) Planar cell polarity, ciliogenesis and neural tube defects. *Human Molecular Genetics*, 15, R227-R234.

- Wallingford, J. B. & R. M. Harland (2002) Neural tube closure requires Dishevelled-dependent convergent extension of the midline. *Development*, 129, 5815-5825.
- Wang, J., N. S. Hamblet, S. Mark, M. E. Dickinson, B. C. Brinkman, N. Segil, S. E. Fraser, P. Chen, J. B. Wallingford & A. Wynshaw-Boris (2006) Dishevelled genes mediate a conserved mammalian PCP pathway to regulate convergent extension during neurulation. *Development*, 133, 1767-1778.
- Wang, J., S. Mark, X. Zhang, D. Qian, S. J. Yoo, K. Radde-Gallwitz, Y. Zhang, X. Lin, A. Collazo, A. Wynshaw-Boris & P. Chen (2005) Regulation of polarized extension and planar cell polarity in the cochlea by the vertebrate PCP pathway. *Nat Genet*, 37, 980-5.
- Westfall, T. A., R. Brimeyer, J. Twedt, J. Gladon, A. Olberding, M. Furutani-Seiki & D. C. Slusarski (2003) Wnt-5/pipetail functions in vertebrate axis formation as a negative regulator of Wnt/beta-catenin activity. *J. Cell Biol.*, 162, 889-898.
- Witze, E. S., E. S. Litman, G. M. Argast, R. T. Moon & N. G. Ahn (2008) Wnt5a Control of Cell Polarity and Directional Movement by Polarized Redistribution of Adhesion Receptors. *Science*, 320, 365-369.
- Wyngaarden, L. A., K. M. Vogeli, B. G. Ciruna, M. Wells, A.-K. Hadjantonakis & S. Hopyan (2010) Oriented cell motility and division underlie early limb bud morphogenesis. *Development*, 137, 2551-2558.
- Yamaguchi, T. P., A. Bradley, A. P. McMahon & S. Jones (1999a) A Wnt5a pathway underlies outgrowth of multiple structures in the vertebrate embryo. *Development*, 126, 1211-23.
- Yamaguchi, T. P., S. Takada, Y. Yoshikawa, N. Wu & A. P. McMahon (1999b) T (Brachyury) is a direct target of Wnt3a during paraxial mesoderm specification. *Genes Dev.*, 13, 3185-90.
- Ybot-Gonzalez, P., D. Savery, D. Gerrelli, M. Signore, C. E. Mitchell, C. H. Faux, N. D. E. Greene & A. J. Copp (2007) Convergent extension, planar-cell-polarity signalling and initiation of mouse neural tube closure. *Development*, 134, 789-799.
- Yoda, A., I. Oishi & Y. Minami (2003) Expression and function of the Ror-family receptor tyrosine kinases during development: lessons from genetic analyses of nematodes, mice, and humans. *J Recept Signal Transduct Res*, 23, 1-15.

CURRICULUM VITAE

John Allen

Education:

Brigham Young University	MS	2013	Physiology and Developmental Biology
Texas State University – San Marcos	BS	2007	Biology/Biochemistry Minor

Research Interests:

Cell and developmental biology – regenerative medicine, gene therapy, genetic engineering, stem cells, cell development, cell differentiation, cell signaling, organogenesis.

Positions Held

Brigham Young University			
Physiology and Developmental Biology	MS student		2010-2013
University of Texas Health Science Center at San Antonio			
Department of Medicine	Summer Researcher		2006

Fellowships, Honors and Awards:

- Texas State Distinguished Biology Major – Spring 2006
- Texas State University Dean's List – Fall 2005, Spring 2007
- Phi Theta Kappa Member
- Midland College Dean's List – Spring 2003
- Brigham Young University Scholarship - 2011
- Brigham Young University Teaching Assistantship – 2010-2013

Techniques:

PCR	DNA Digestion
Agarose Gel Electrophoresis	Plasmid Subcloning
RNA Extraction and Purification	Plasmid Purification
Reverse Transcription	Cell Transfection
Chick embryo bead implantation	Sonoporation

Research Experience:

Graduate

Notch-Delta pathway in early chick development. Dr. Michael Stark, Brigham Young University, 2007

Mechanisms of limb outgrowth and patterning in mouse and signaling pathways that regulate directional migration and oriented cell division during vertebrate embryogenesis. Dr. Jeffery Barrow, Brigham Young University 2007

Cellular mechanisms of endothelial-mesenchymal transition. Dr. Marc Hansen, 2010

Upregulation of receptors for advanced glycation endproducts (RAGE) and lung

development. Dr. Paul Reynolds, 2010

The role of Wnt5b signaling through non-canonical pathways in embryonic axis outgrowth.

Dr. Jeffery Barrow, 2010

FGF signals from the apical ectodermal ridge (AER) induce a Wnt5a gradient and limb mesenchymal cell outgrowth. Dr. Jeffery Barrow, 2010

Sonic Hedgehog secreted from the zone of polarizing activity (ZPA) in gradient fashion mediates digit number through Gli3R repression. Dr. Jeffery Barrow, 2011

Undergraduate:

Auxin receptor mutation's effect on mustard plant development. Dr. Nihal Dharmasiri, Texas State University, 2007

Effect of Hamster Nramp on iNOS Production in Mouse Macrophage Cells Compared to Mouse Nramp. Dr. Peter Melby, University of Texas Health Science Center at San Antonio, 2006

Molecular Characterization of PDE1 Gene in Bluegill Sunfish. Dr. Dana Garcia, Texas State University – San Marcos, 2006

Poster Presentation

John Allen, Omar Saldarriaga and Peter Melby. Effect of Hamster Nramp on iNOS Production in Mouse Macrophage Cells Compared to Mouse Nramp. University of Texas Health Science Center at San Antonio. (2006).

John Allen, Jed J. Kendall, Jared Barrot, Fanxin Long, Andrew P. McMahon, Jeffery R. Barrow. Wnt5a and Wnt5b function redundantly via noncanonical pathways to extend the embryonic axis. (2011) 70th annual meeting of the Society of Developmental Biology, Chicago, IL.

John Allen, Jed J. Kendall, Jared Barrot, Fanxin Long, Andrew P. McMahon, Jeffery R. Barrow. Wnt5a and Wnt5b function redundantly via noncanonical pathways to extend the embryonic axis. (2013) Southwest Regional Meeting of the Society of Developmental Biology, Salt Lake City, UT.

Teaching Experience

Lab Instructor, Physiology 305, Brigham Young University. 2010-2013

Lab Instructor, Anatomy and Physiology I, Midland College. 2009